



HAL
open science

Electrical properties of self-assembled InAs/InAlAs quantum dots on InP

N. Hamdaoui, R. Ajjel, H. Maaref, B. Salem, G. Bremond, M. Gendry

► **To cite this version:**

N. Hamdaoui, R. Ajjel, H. Maaref, B. Salem, G. Bremond, et al.. Electrical properties of self-assembled InAs/InAlAs quantum dots on InP. *Semiconductor Science and Technology*, 2010, 25 (6), pp.065011. 10.1088/0268-1242/25/6/065011 . hal-00623432

HAL Id: hal-00623432

<https://hal.science/hal-00623432>

Submitted on 16 Mar 2023

HAL is a multi-disciplinary open access archive for the deposit and dissemination of scientific research documents, whether they are published or not. The documents may come from teaching and research institutions in France or abroad, or from public or private research centers.

L'archive ouverte pluridisciplinaire **HAL**, est destinée au dépôt et à la diffusion de documents scientifiques de niveau recherche, publiés ou non, émanant des établissements d'enseignement et de recherche français ou étrangers, des laboratoires publics ou privés.



Distributed under a Creative Commons Attribution - NonCommercial 4.0 International License

Electrical properties of self-assembled InAs/InAlAs quantum dots on InP

N Hamdaoui¹, R Ajjel^{1,6}, H Maaref², B Salem³, G Bremond⁴ and M Gendry⁵

¹ Laboratoire d'énergétique et de transfert thermique et massique LETTM, Ecole supérieur des Sciences et de la Technologie Hammam Sousse, 4011, Tunisia

² Département de physique, Faculté des Sciences, Laboratoire de physique des Semiconducteurs et des Composants Electroniques (LPSCE), 5019 Monastir, Tunisia

³ Laboratoire des Technologies de la Microélectronique (LTM), UMR CNRS, CEA-Grenoble, 17 Rue des Martyrs, F-38054 Grenoble, France

⁴ Institut des Nanotechnologies de Lyon (UMR5270/CNRS), Site INSA de Lyon, Bâtiment Blaise Pascal, 7 Avenue J. Capelle, 69621 Villeurbanne, France

⁵ Institut des Nanotechnologies de Lyon (UMR5270/CNRS), Site Ecole Centrale de Lyon, 36 avenue Guy de Collongue, 69134 Ecully, France

E-mail: hamdaoui nejeh@yahoo.fr

Abstract

The characteristics of InAs self-assembled quantum dots (QDs) grown on InAlAs/InP (001) have been investigated by capacitance–voltage (C – V) measurements and deep-level transient spectroscopy (DLTS). The depth profile of the apparent electron concentration obtained by C – V measurements shows significant carrier accumulation around the position of the InAs QDs plane. In addition to the D_1 – D_5 traps, which are commonly detected in InAlAs layers grown on InP by molecular beam epitaxy (MBE), DLTS investigations show three InAs-related levels located at about 76, 202 and 246 meV below the InAlAs conduction band edge. The applied field is found to significantly enhance tunnel emission processes as seen in the broadening of the peaks with increasing reverse bias. The results suggest that defects in the material barrier can enhance electron tunnelling through barriers.

1. Introduction

The research on low-dimensional structures such as quantum dots (QDs) shows promising properties in future optoelectronic devices. A great deal of attention has been paid to the growth [1–3], the electronic properties [4–6] and the transport mechanisms [7–9].

Self-assembled InAs quantum dots (QDs), quantum dashes (QDas) and quantum wires (QWRs) grown by the Stranski–Krastanow (S–K) mode on a InP substrate have attracted much attention due to their application in semiconductor lasers at 1.55 μm and long-wavelength infrared photodetectors [10, 11]. Most of the work is focused on the optical properties of InAs/InP nanostructures grown on

the InP substrate [12–16]. Some studies have been devoted to the optical properties of the InAs/InAlAs nanostructures grown on InP [17, 18]. The infrared absorption spectra and photoconductive spectra have been investigated [19–21]. Less attention has been devoted to the electrical properties of these InP-based InAs/InAlAs nanostructures [22, 23].

For the development of optoelectronic devices based on these heterostructures, it is crucial to study their electronic properties in connection with transport mechanisms in the nanostructures. To this end, a number of techniques have been employed, such as deep level transient spectroscopy (DLTS). DLTS has been proved to be a powerful tool to probe the electronic properties of QD systems [24]. Further investigations are therefore required to clarify the emission and capture processes of QD-related levels as well as the influence of the growth conditions on the generation of electrically active defects in the QD region.

⁶ Present address: Ecole supérieure des sciences et de la technologie, 4011 Hammam Sousse, Sousse Tunisia.

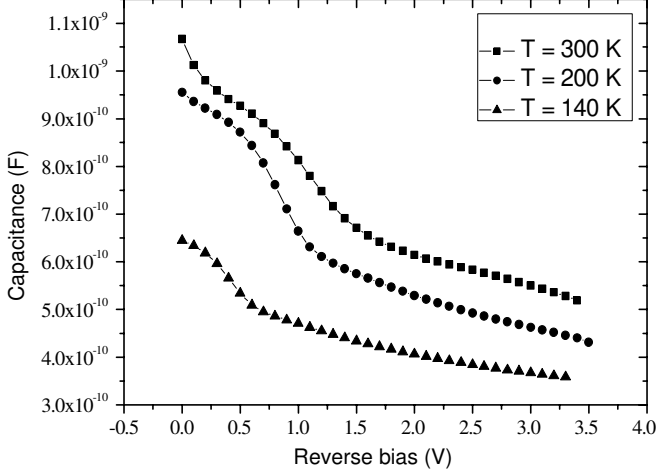


Figure 1. C - V measurements performed at $T = 300, 200,$ and 140 K for the InAs QDs embedded in n-type InAlAs matrix.

In this study, we analysed the energy level of the InAs/InAlAs/InP QD system using C - V and DLTS measurements, as well as the influence of the applied field on the emission process. Qualitative information on the electron emission process from the dots is obtained from DLTS measurements. Our results suggest that defects in the material barrier can contribute to the enhancement of electron tunnelling through barriers.

2. Results and discussions

The investigated sample was grown on an n^+ -doped InP (001) substrate by solid source molecular beam epitaxy (SSMBE). It consisted of a $0.4 \mu\text{m}$ thick $\text{In}_{0.52}\text{Al}_{0.48}\text{As}$ (InAlAs) buffer followed by 0.9 nm of InAs. InAlAs buffer surface preparation and InAs growth conditions were adjusted to favour dot-like rather than wire-like islands [25]. Since the sample was designed for electrical characterization, the buffer was Si doped at $3 \times 10^{16} \text{ cm}^{-3}$. The InAs thickness of three monolayers (ML) was just above the 2D/3D growth mode transition detected by reflection high electron energy diffraction at 2.5 ML. Then, a 10 nm thick non-intentionally doped (n.i.d.) InAlAs layer, a 170 nm thick Si-doped InAlAs layer at $3 \times 10^{16} \text{ cm}^{-3}$, and a 20 nm thick n.i.d. InAlAs layer were grown. Schottky contacts were fabricated by evaporating 20 nm of gold (Au) onto InAlAs through a contact mask. A back ohmic contact was formed with Au-Ge-Ni alloy on the n^+ substrate. Details of the growth process and atomic force microscopy (AFM) images of the InAs QDs are published elsewhere [26–29]. We noted that the histogram of the dot heights obtained with AFM measurements revealed a broad height distribution centred at 1.5 nm with a full width at half maximum (FWHM) of 0.6 nm (see the inset of figure 1 in [26]).

The QD sample studied in this work was investigated earlier by photoluminescence measurements carried out at 10 K as a function of the excitation power. The spectrum obtained (not shown here) confirms the presence of ground and excited states, as also reported for similar structures [22, 30].

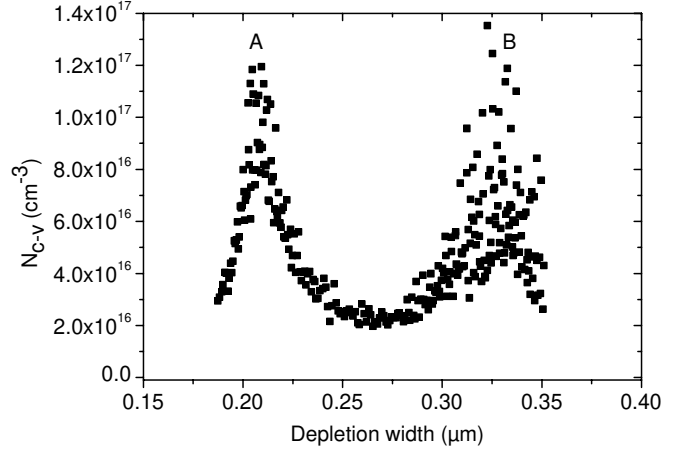


Figure 2. Carrier distribution profile.

Figure 1 shows the C - V profiles of the QD sample measured at different temperatures using a test signal of 1 MHz . We observe a plateau in the C - V curve, which indicates that the boundary of space charge region is located at the QD plane where a large concentration of confined electrons block further extension of the space charge region. As also shown in figure 1, two steps are resolved in the capacitance plateau. They were assigned to the charging of the QD ground and excited states, which was confirmed by the DLTS measurements discussed below.

As the reverse bias voltage increases, the Fermi level E_f gradually moves down through the electronic states of the QDs. The space charge region extends over the QD plane so that the electrons in the QDs are completely pumped out. Further, it should be noted that for temperature below 300 K , the modulation of the C - V curve is shifted to smaller reverse biases resulting in a shortened plateau-like structure. This behaviour is due to tunnelling effects [31]. Using these C - V measurements, the spatial distribution of the electrons along the growth direction [$N_{c-v}(W)$] was calculated by the usual equations for the C - V profile:

$$N_{c-v} = \frac{C^3}{qA^2\epsilon(dC/dV)},$$

and

$$W = \frac{\epsilon A}{C},$$

where A represents the surface of the Schottky contact, q is the elementary charge and ϵ is the dielectric constant.

The N_{c-v} profile (figure 2) shows a strong peak A at about $0.2 \mu\text{m}$. Besides the peak A, another broad peak B appears at about $0.32 \mu\text{m}$. These carrier accumulation peaks can be originated by carrier redistribution by energy bands of QDs. The QDs have discrete energy states, which are lower than the conduction band of InAlAs. Therefore, carriers are easily formed on these energy levels.

We should note here that, on the basis of the C - V analysis, Saad *et al* have studied the electronic properties of InAs QDs grown on n- and p-type InAlAs/InP matrices [32]. They found that holes are more confined than electrons.

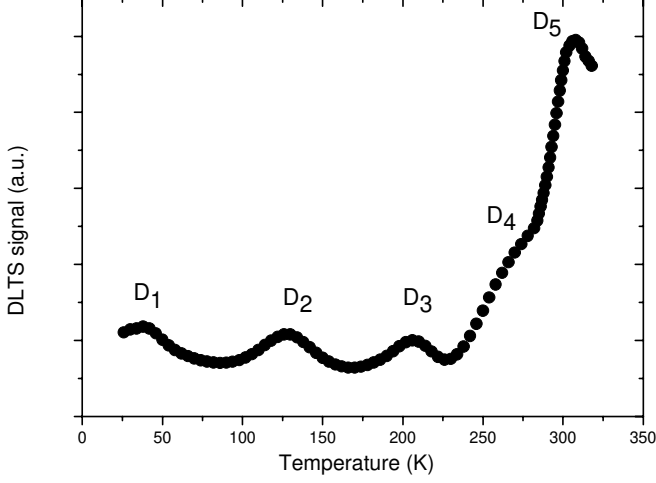


Figure 3. DLTS spectra obtained for the reference sample InAlAs/InP. Recording conditions: emission rate: 426 s^{-1} , reverse bias: 2 V, filling pulse: 0 V, and filling time t_p : 0.5 ms.

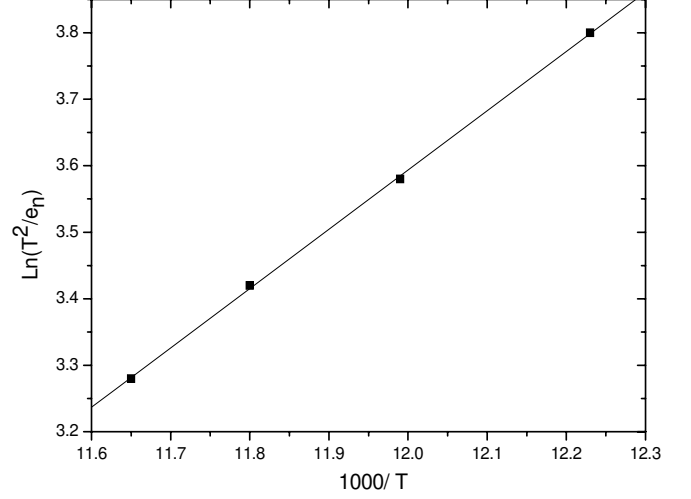


Figure 5. Variation of $\ln(T^2/e_n)$ versus $1000/T$ for the d signal.

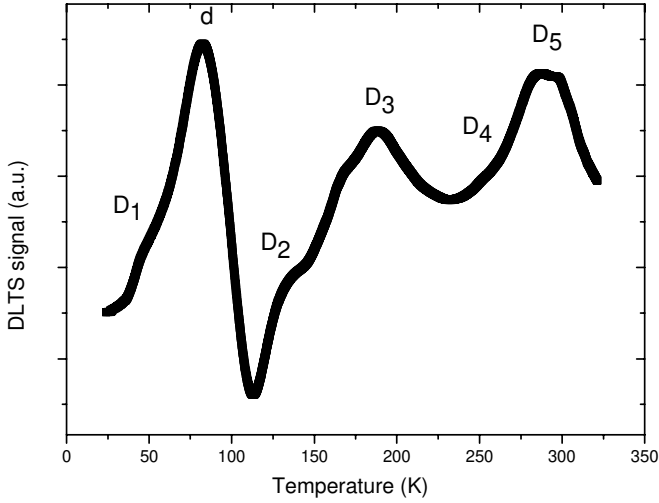


Figure 4. DLTS spectra obtained for the QD sample. Recording conditions: emission rate: 426 s^{-1} , reverse bias: 1 V, filling pulse: 0 V and filling time t_p : 0.5 ms.

To identify the origin of the different peaks observed in the DLTS spectrum, we have studied a structure without QDs. In figure 3, the DLTS measurement of this InAlAs/InP reference sample at the rate window $e_n = 426 \text{ s}^{-1}$ is displayed. During the measurement, the reverse bias V_r was 2 V, the pulse bias V_p was 0 V and the pulse width (t_p) was fixed to 0.5 ms. The electrons are emitted as a consequence of thermal activation. The thermal emission rate e_n is written as [33]

$$e_n = \delta T^2 \sigma \exp\left(\frac{-E_a}{kT}\right),$$

where E_a is the activation energy, σ is the capture cross section for $T = \infty$ and δ is a temperature-independent constant.

Five electron traps D1 to D5 are clearly resolved in the spectra. The energies determined from the thermal emission are discussed in detail in [34].

In figure 4, the characteristic DLTS spectrum of the QD sample obtained with $V_p = 0 \text{ V}$, $V_r = 1 \text{ V}$, $t_p = 0.5 \text{ ms}$ and

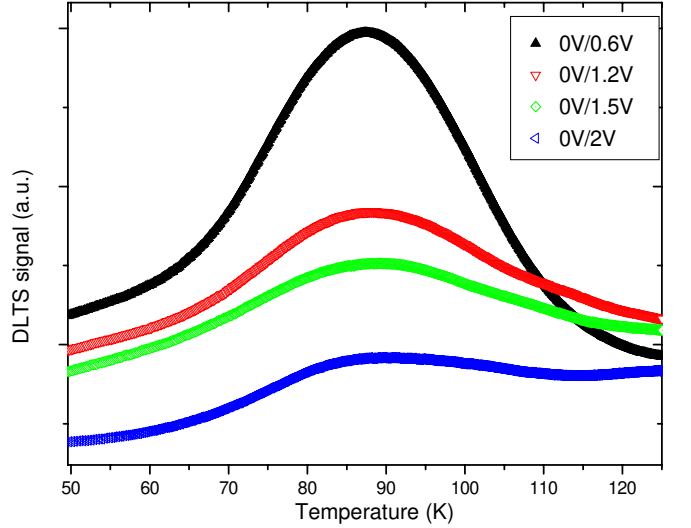


Figure 6. DLTS spectrum obtained for the InAs QD structure for different reverse bias.

$e_n = 426 \text{ s}^{-1}$ is reported. As can be seen, the peaks labelled as D1 to D5 are present in both samples. Based on their emission signatures and on a comparison with data obtained in [34, 35], these traps may result from defects of the InAlAs/InP heterojunction.

The peak centred at about 80 K, which is detected only on the QD sample and only when the region explored by DLTS containing the InAs QDs can be obviously related to the QDs. From an Arrhenius plot of the DLTS peak position for varying thermal emission rate e_n , we obtain an apparent energy E_d equal to 76 meV and a capture cross section equal to $1.3 \times 10^{-12} \text{ cm}^2$ (figure 5). The observed activation energy agreed well with the energy difference between the QD d shell and the InAlAs conduction band edge as predicted from a simple two-band $\mathbf{k} \cdot \mathbf{p}$ model (which takes into account the strong nonparabolicity in InAs) and photoinduced absorption spectroscopy for the given QD geometry [30].

We proceed to explore the consequence of increased reverse bias on the d shell signal. Figure 6 shows the DLTS

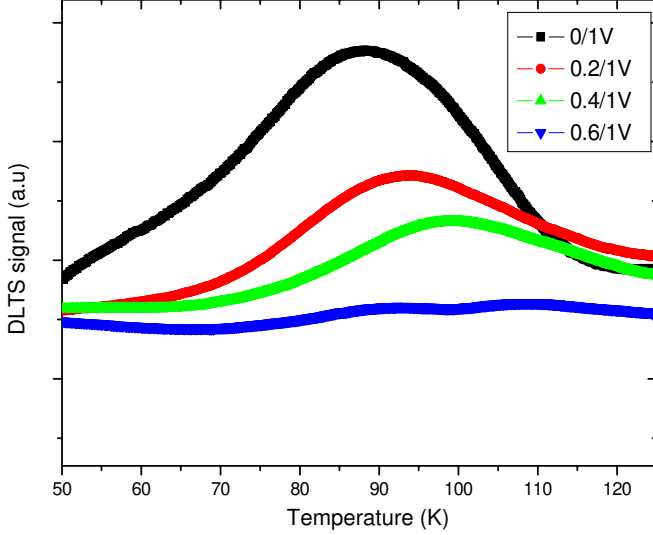


Figure 7. DLTS spectrum obtained for the InAs QD structure for different filling bias.

signals for various reversed bias voltages. We find that the peaks shift to higher temperature and gradually become broad with increasing reverse bias. The amplitude of the peaks is found to decrease with enhanced reverse bias. This behaviour is related to the carrier concentration in the d excited states. The electron concentration can be identified by the position of the Fermi level. It moves with increasing reverse bias across higher energy levels and also detects electron emission from deeper levels of the dots. On the other hand, the tunnelling probability of electrons increases with the applied bias, so the amplitude of DLTS peaks will decrease with the increase of reverse bias. Accordingly, the DLTS peaks shift to high temperature, and the peaks become broad gradually.

Applying a fixed reverse bias $V_r = 1$ V and decreasing the filling pulse bias V_p (figure 7), the DLTS signal resembles the structure previously discussed, namely, a decrease in overall amplitude due to an increase in pulse bias. For a pulse bias of $V_p = 0.6$ V, no DLTS signal is visible. As the pulse bias is decreased, the amplitude of the DLTS peak increases and shifts towards lower temperature. This behaviour may be explained by partial filling of the electron energy levels in the InAs QDs. For high filling pulse biases, the depletion region during the pulse is only weakly decreased and only the d level of the larger QDs in the ensemble are situated below the Fermi level. Hence, only a few electrons can enter the QDs occupying the d level, which leads to suppression in the DLTS signal. For decreasing the pulse bias, an increasing number of electrons can be filled into the d level, leading to an increasing contribution of multi-electron interaction to the total energy. This contribution results from the Coulomb charging energy. This effect may explain the observed shifts of the peak towards lower temperatures.

By a proper choice of experimental parameters, the intrinsic peaks of the discrete energy levels of the QDs should be observed. In figure 8, DLTS spectra for an emission rate of $e_n = 426$ s⁻¹ for a reverse bias $V_r = 3$ V and a pulse voltage of $V_p = 1.5$ V are displayed. The pulse duration was 0.5 ms.

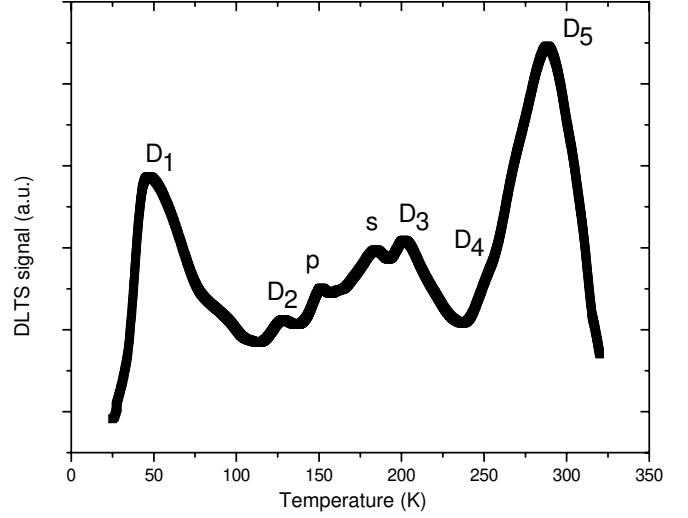


Figure 8. DLTS spectra obtained for the QD sample with $V_p = 1.5$ V and $V_r = 3$ V.

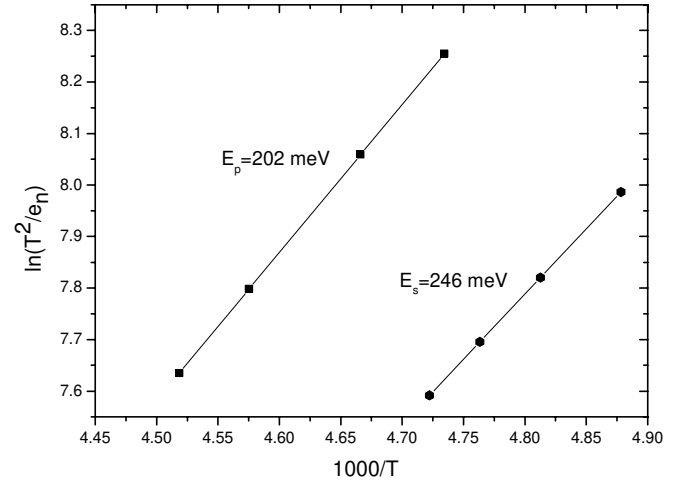


Figure 9. Variation of $\ln(T^2/e_n)$ versus $1000/T$ for the p and s signals.

Two peaks p and s are observed, which do not appear in the DLTS curve of the reference sample. Obviously, peaks p and s are due to the electron emissions from the dots.

Using thermal emission processes, we found that the standard Arrhenius evaluation of temperature-dependent emission rate obtained from the DLTS measurement yielded apparent thermal activation energies, and emission cross sections were obtained as 202 meV and 246 meV, and 2.6×10^{-13} and 3.8×10^{-13} cm², respectively (figure 9). Our results are close to many other published data about the electronic levels of QDs measured by infrared spectroscopy and photocurrent spectroscopy [11, 30].

For voltages lower than 3 V, no signal is seen because the Fermi level is positioned above the s and p QD energy levels for these voltages. By increasing the voltage to 3 V, the p shell of the QD electrons starts emitting signals. When the Fermi level is low enough to empty also the s shell, a signal component is added. While increasing the measurement

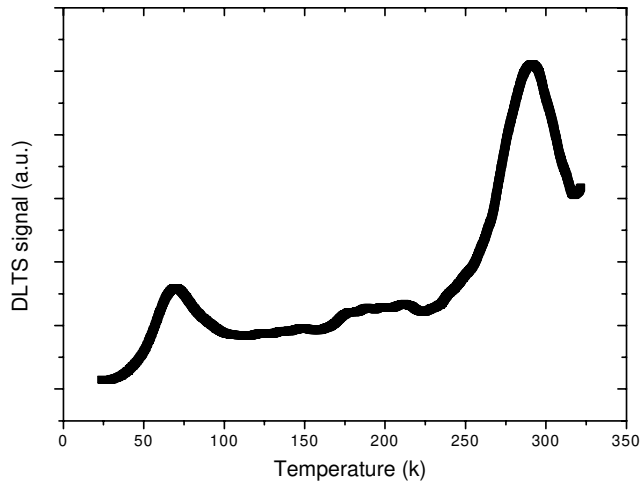


Figure 10. DLTS spectra for InAs QD structure with $V_p = 1.5$ V and $V_r = 3.5$ V.

temperature, the discrete energy levels corresponding to different thermal ionization energies are gradually observed in the DLTS spectrum. Thus, we attribute these signals to the emission of electrons from the first excited state (p) and the ground state (s).

Additional measurements were made on the QD sample to determine the consequences of increased reverse bias on the emission processes of electrons from p and s levels. In figure 10, the pulse voltage is kept at the same value of 1.5 V, while the reverse bias is varied from 3 to 3.5 V. We observed a plateau-like DLTS feature as shown in figure 10. The p and s peaks disappeared. Such QD DLTS peaks are well resolved only at a certain bias voltage. This is because when $V_r > 3$ V the emission is dominated more by tunnelling, which is rather temperature independent and therefore less visible in the DLTS spectra. We attribute this plateau feature to the tunnelling effect in QD. The tunnel emission is strongly enhanced and quickly dominates, as can be seen from the DLTS signal.

A similar feature was reported by many other studies in InAs/GaAs QDs [36–39]. Our results suggest that defects enhance electron tunnelling through barriers. This defect enhancement is likely the reason for the strong and quick dominance of tunnel emission that is found to accompany a weak increase in reverse bias.

For electronic device applications, the existence of states that are much deeper than the intrinsic QD states could be utilized to design memory devices. Balocco *et al* demonstrated a fully electrically controlled, room temperature memory device where InAs QDs were embedded in a modulation-doped high electron mobility transistor structure [40]. The coexistence of similar deep levels in the QD layer was confirmed by the experiments using different gate biases to control the transfer of electrons between the deep levels and two-dimensional electron gas. In such devices, the slow charging of the deep levels, rather than the emission or the discharging process, provided a long memory time even at room temperature.

3. Conclusions

In conclusion, it has been shown that C - V and DLTS measurements carried out on InAs/InAlAs QDs on InP provide information on the energy levels induced by the InAs QDs. Strong changes were observed in DLTS spectra when studied as a function of the applied voltage. These lead us to suggest that defects contribute in the enhancement of electron tunneling through the barriers.

References

- [1] Pan E, Sun M, Chung P W and Zhu R 2007 *Appl. Phys. Lett.* **91** 193110
- [2] Liang B-L, Wang Z-M, Wang X-Y, Lee J-H, Mazur Y I, Shih C-K and Salamo G J 2008 *ACS Nano* **2** 2219
- [3] Sablon K A, Lee J H, Wang Z M, Shultz J H and Salamo G J 2008 *Appl. Phys. Lett.* **92** 203106
- [4] Li S-S, Xia J-B, Yuan Z L, Xu Z Y, Ge W, Wang X R, Wang J and Chang L L 1996 *Phys. Rev. B* **54** 11575
- [5] Barker J K, Warburton R J and O'Reilly E P 2004 *Phys. Rev. B* **69** 035327
- [6] Lee J H, Wang Z M, Dorgan V G, Mazur Y I, Ware M E and Salamo G J 2009 *J. Appl. Phys.* **106** 073106
- [7] Li S-S, Abliz A, Yang F-H, Niu Z-C, Feng S-L and Xia J-B 2002 *J. Appl. Phys.* **92** 6662
- [8] Chakrabarti S, Stiff-Roberts A D, Bhattacharya P, Gunapala S, Bandra S, Rafol S B and Kennerly S W 2004 *IEEE Photonics Technol. Lett.* **16** 1361
- [9] Hoglund L, Holtz P O, Pettersson H, Asplund C, Wang Q, Almqvist S, Smulk S, Petini E and Andersson J Y 2008 *Appl. Phys. Lett.* **93** 103501
- [10] Kim J S, Lee J H, Hong S U, Han W S, Kwack H S, Lee C W and Oh D K 2004 *Appl. Phys. Lett.* **85** 1033
- [11] Finkman E, Maimon S, Immer V, Bahir G, Schacham S E, Fossard F, Julien F H, Brault J and Gendry M 2001 *Phys. Rev. B* **63** 045323
- [12] Bierwagen O and Masselink W T 2005 *Appl. Phys. Lett.* **86** 113110
- [13] Alen B, Martinez-Pastor J, Gonzalez L, Garcia J M, Molina S I, Ponce A and Garcia R 2002 *Phys. Rev. B* **65** 241301
- [14] Zhang Z H, Xu C F, Hsieh K C and Cheng K Y 2005 *J. Cryst. Growth* **278** 61
- [15] Salem B, Benyattou T, Guillot G, Bruchevalier C, Bremond G, Monat C, Hollinger G and Gendry M 2002 *Phys. Rev. B* **66** 193305
- [16] Salem B, Bremond G, Benyattou T, Bruchevalier C, Guillot G, Monat G, Gendry M, Hollinger G, Jbeli A and Marie X 2003 *Physica E* **17** 124–6
- [17] Hjiri M, Hassen F, Maaref H, Salem B, Bremond G, Marty O, Brault J and Gendry M 2003 *Physica E* **17** 180
- [18] Lei W, Chen Y H, Wang Y L, Huang X Q, Zhao C, Liu J Q, Xu B, Jin P, Zeng Y P and Wang Z G 2006 *J. Cryst. Growth* **286** 23
- [19] Finkman E, Maimon S, Immer V, Bahir G, Schacham S E, Gauthier-Lafaye O, Herriot S, Julien F H, Gendry M and Brault J 2000 *Physica E* **7** 139
- [20] Fossard F, Helman A, Julien F H, Gendry M, Brault J, Peronne E, Alexandrou A, Schacham S E and Finkman E 2003 *Physica E* **17** 82
- [21] Fossard F, Julien F H, Peronne E, Alexandrou A, Brault J and Gendry M 2001 *Infrared Phys. Technol.* **42** 443
- [22] Ajjel R, Baira M, Gassoumi M, Maaref H, Salem B, Brémond G and Gendry M 2006 *Semicond. Sci. Technol.* **21** 311–5
- [23] He J, Xu B and Wang Z G 2004 *Appl. Phys. Lett.* **84** 5237

- [24] Engstrom O and Kaniewska M 2008 *Nanoscale. Res. Lett.* **3** 179
- [25] Brault J, Gendry M, Grenet G, Hollinger G, Olivares J, Salem B, Benyattou T and Brémond G 2002 *J. Appl. Phys.* **92** 506
- [26] Weber A, Gauthier-Ilafaye O, Julien F H, Brault J, Gendry M, Désières Y and Benyattou T 1999 *Appl. Phys. Lett.* **74** 413
- [27] Zhao F A, Chen Y H, Ye X L, Xu B, Jin P, Wu J, Wang Z G and Zhang C L 2005 *J. Cryst. Growth* **273** 494
- [28] Lei W, Chen Y H, Jin P, Ye X L, Wang Y L, Xu B and Wang Z G 2006 *Appl. Phys. Lett.* **88** 063114
- [29] Lei W, Ren Y L, Wang Y L and Li Q 2009 *J. Cryst. Growth* **311** 4632
- [30] Fossard F, Helman A, Fishman G, Julien F H, Brault J, Gendry M, Péronne E, Alexandrou A, Schacham S E, Bahir G and Finkman E 2004 *Phys. Rev. B* **69** 155333
- [31] Gonschorek M, Schmidt H, Bauer J, Benndorf G, Wagner G, Cirlin G E and Grundmann M 2006 *Phys. Rev. B* **74** 115312
- [32] Saad O, Baira M, Ajjel R, Maaref H, Salem B, Brémond G and Gendry M 2008 *Microelectron. J.* **39** 7–11
- [33] Lang D V 1974 *J. Appl. Phys.* **45** 3023
- [34] Ajjel R, Baira M, Hellara J, Maaref H, Salem B, Brémond G and Gendry M 2007 *Physica B* **391** 18–21
- [35] Hong W P, Dhar S, Bhattacharya P K and Chin A 1987 *J. Electron. Mater.* **16** 271
- [36] Schulz S, Schramm A, Heyn C and Hansen W 2006 *Phys. Rev. B* **74** 033311
- [37] Schramm A, Schulz S, Heyn C and Hansen W 2008 *Phys. Rev. B* **77** 153308
- [38] Kapteyn C M A, Lion M, Heitz R, Brunkov P N, Volvik B V, Konnikov S G, Kovsh A R, Ustinov V M and Bimberg D 2000 *Appl. Phys. Lett.* **76** 1573
- [39] Engstrom O, Kaniewska M, Kaczmarczyk M and Jung W 2007 *Appl. Phys. Lett.* **91** 133117
- [40] Balocco C, Song A M and Missous M 2004 *Appl. Phys. Lett.* **85** 5911